



**Michigan  
Technological  
University**

Michigan Technological University  
**Digital Commons @ Michigan Tech**

---

Dissertations, Master's Theses and Master's Reports

---

2020

## Measurement of current distribution in the land channel direction of a proton exchange membrane fuel cell

Chinmay Kulkarni

*Michigan Technological University, cakulkar@mtu.edu*

Copyright 2020 Chinmay Kulkarni

---

### Recommended Citation

Kulkarni, Chinmay, "Measurement of current distribution in the land channel direction of a proton exchange membrane fuel cell", Open Access Master's Report, Michigan Technological University, 2020.  
<https://doi.org/10.37099/mtu.dc.etdr/976>

Follow this and additional works at: <https://digitalcommons.mtu.edu/etdr>



Part of the [Automotive Engineering Commons](#), and the [Energy Systems Commons](#)

MEASUREMENT OF CURRENT DISTRIBUTION IN THE LAND CHANNEL  
DIRECTION OF A PROTON EXCHANGE MEMBRANE FUEL CELL

By

Chinmay A. Kulkarni

A REPORT

Submitted in partial fulfillment of the requirements for the degree of

MASTER OF SCIENCE

In Mechanical Engineering

MICHIGAN TECHNOLOGICAL UNIVERSITY

2020

© 2020 Chinmay A. Kulkarni

This report has been approved in partial fulfillment of the requirements for the Degree of MASTER OF SCIENCE in Mechanical Engineering.

Department of Mechanical Engineering-Engineering Mechanics

Report Advisor:*Dr. Kazuya Tajiri*

Committee Member:*Dr. Jeffrey Allen*

Committee Member:*Dr. Radheshyam Tewari*

Department Chair:*Dr. William Predebon*

## Table of Contents

List of figures .....	iv
List of tables .....	vi
Abstract .....	vii
1 Introduction.....	1
1.1 Classification of Fuel Cells .....	1
1.2 Components of PEMFC .....	7
2 Operation Principle of PEMFC.....	13
2.1 Performance of PEMFC .....	14
3 Segmentation of PEMFC .....	18
4 Importance of Land Channel Geometry: Literature Review .....	21
4.1 Effect on Water Distribution .....	22
4.2 Effect on Current Distribution.....	23
5 Experimental Setup.....	26
5.1 Design of Segmented Anode Flow Channel .....	26
5.2 Design of Current Distribution Measurement System .....	27
5.3 Preparation of Membrane Electrode Assembly (MEA) .....	28
5.4 Assembly of Segmented Cell .....	30
6 Results and Discussions.....	34
7 Conclusions and Future Work .....	41
8 References.....	42

## List of figures

Figure 1.1. Schematic Representation of a PEMFC. ....	8
Figure 1.2. Chemical Structure of Nafion membrane.....	9
Figure 1.3. SEM images of catalyst coated membrane.....	11
Figure 1.4. SEM image of Toray 060 carbon paper (left) and E-Tek carbon cloth (right)12	
Figure 2.1 Working principle of PEMFC. ....	13
Figure 2.2. Sample polarization curve of PEMFC.....	14
Figure 3.1. Segmented current collector.....	18
Figure 4.1. Schematic diagram of land channel geometry in the flow field of a PEMFC.21	
Figure 4.2. Water distribution in GDL with respect to land channel geometry at 80°C and 2.5 A/cm <sup>2</sup> current density. ....	22
Figure 4.3. Current density distribution for interdigitated flow pattern .....	24
Figure 4.4. Local current density distribution for dry and flooded.....	25
Figure 5.1. Segmented anode side current collector.....	26
Figure 5.2. Experimental setup for measurement of local current density .....	28
Figure 5.3. Schematic representation of MEA preparation a) Catalyst coated membrane sandwiched between anode and cathode assembly b) cross section of MEA.....	29
Figure 5.4. Catalyst coated membrane in the hot press. ....	30
Figure 5.5. Assembly of segmented cell representing a) Anode end plate b) Segmented anode current collector c) Catalyst coated membrane d) Cathode GDL e) Cathode bipolar plate f) Cathode current collector g) Cathode end plate.....	31
Figure 5.6. Components of Segmented cell assembly .....	32
Figure 5.7. Cross section view of segmented cell assembly.....	32
Figure 6.1. Performance of cell at dry, moderate and wet humidity conditions.....	34
Figure 6.2. Local current distribution for dry condition .....	36
Figure 6.3. Local current distribution in wet condition .....	37

Figure 6.4. Local current density distribution in moderate humidity setup.....38

Figure 6.5. Performance of individual segment for moderate humidity condition.....39

## List of tables

Table 1 Classification of Fuel cells.....	7
Table 2. NEDO preconditioning parameters for PEMFC.....	33
Table 3. Testing Conditions for the measurement of the local current density in the land channel direction. ....	33

## Abstract

A fully functional proton exchange membrane fuel cell with single land channel geometry on the cathode and segmented anode current collector with 9 mm<sup>2</sup> active area with a 350µm spatial resolution was utilized to measure the local current distribution in the land channel direction. A distinguished printed circuit board approach was used for the data acquisition to adapt to any flow field design.

Performance of this segmented cell was examined at dry, wet and moderate humidity settings to study the water transport phenomenon in the PEMFC. In the dry condition at 60° C with 0% relative humidity, the non-uniform water production and dehydrated membrane revealed high current localization under the land region. Conversely, in the wet condition at 60° C with 80% relative humidity, due to the severe flooding in the catalyst layer resulted in very small limiting current density under the channel region. Individual segment performance analysis for the moderate settings at 60° C with 60% relative humidity displayed the uniform current distribution at higher cell potential whereas irregular local current generation at low cell voltages due to higher water accumulation under the land region.



# 1 Introduction

A fuel cell is an electrochemical energy conversion device which uses the chemical energy from an external fuel source (mostly hydrogen) and converts it to the electrical energy with the help external oxidizing agent (mostly oxygen) by undergoing redox reactions. A fuel cell can continuously produce electricity as far as the fuel is supplied.

An assembly of fuel cell consists of an anode, a cathode, and a membrane electrode assembly (MEA). At anode, a fuel is supplied which undergoes an oxidation reaction separating ions and electrons. The ions are passed through the electrolyte membrane while electrons are released in the external circuit generating electric current. At cathode, the oxidizing agent is supplied which undergoes reduction reaction with the help of electrons and ions to produce water. The detailed operating principle of a fuel cell is discussed later in the report. All the results and discussions presented in this report are totally based on the study of proton exchange membrane fuel cell (PEMFC).

## 1.1 Classification of Fuel Cells

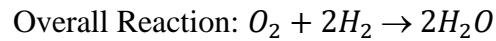
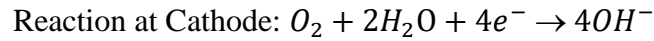
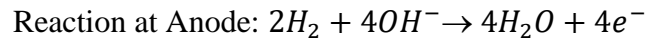
Fuel cells can be classified based on the type of electrolyte used, operating temperature, and its application areas. Discussed below are some of the primary types of fuel cell.

### a. Alkaline Fuel Cells (AFC)

Alkaline fuel cells use alkaline solutions, such as Potassium Hydroxide (KOH) solution as an electrolyte and non-precious metals as electrodes. In AFC, the rate of the electrochemical reaction is fast and thus provides a very high efficiency.

These fuel cells don't need continuous supply of electrolyte due to recirculating electrolyte generation.

Reactions in AFC:

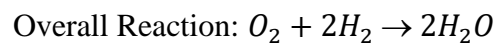
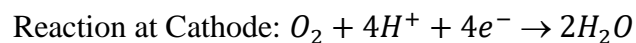
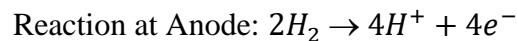


The major drawback of the AFC is that it is not tolerant to Carbon dioxide (CO<sub>2</sub>). The minimum amount of CO<sub>2</sub> in the air can lead to poisoning and can drastically affect the overall efficiency due to carbonate formation. Low water handling capacity and increased corrosion are also some of the other problems faced during the operation of AFC.

b. Phosphoric Acid Fuel Cells (PAFC)

Phosphoric acid fuel cells use liquid phosphoric acid (H<sub>3</sub>PO<sub>4</sub>) as an electrolyte and platinum activated carbon electrodes.

Reactions in PAFC:

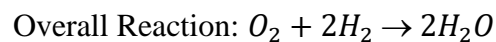
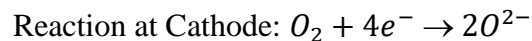
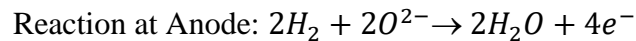


The use of precious metal catalysts such as Platinum are poisoned due to Carbon monoxide (CO) formation which greatly affects the life and overall performance of the cell. However, operating the fuel cell at higher temperatures can minimize this problem.

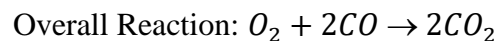
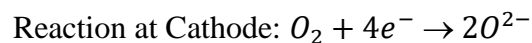
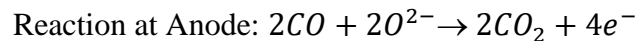
c. Solid Oxide Fuel Cells (SOFC)

Solid oxide fuel cells use a non-porous ceramic as an electrolyte. These fuel cells are operated at very high temperatures (800-1000°C) and thus does not require any precious metal catalysts. SOFC can use wide range of fuels such as Carbon monoxide, hydrogen, etc.

Reactions in SOFC: Using Hydrogen as a fuel



Reactions in SOFC: Using Carbon monoxide as a fuel



The operation of SOFC provides a lot of high-quality waste heat which can be used for wide range of applications. Being operated at a high temperature can lead to leakage in the cell due to the variation in the thermal expansion coefficients of the materials used.

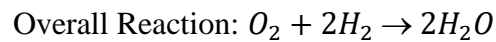
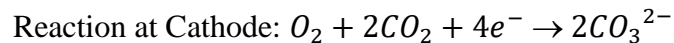
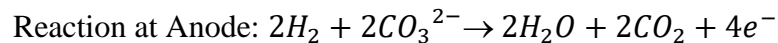
d. Molten Carbonate Fuel Cells (MCFC)

Molten carbonate fuel cells use molten carbonate salts mixture as an electrolyte.

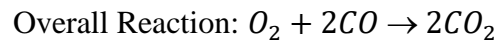
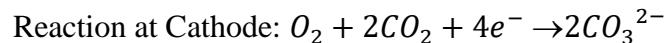
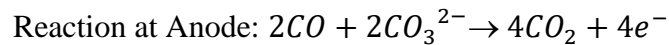
These fuel cells are also operated at a considerably high temperature (650°C) and hence non-precious metals can be used as catalysts, thus, reducing the cost.

Similar to SOFC, MCFC can also use carbon monoxide as a fuel.

Reactions in MCFC: Using Hydrogen as a fuel



Reactions in MCFC: Using Carbon monoxide as a fuel



Due to the operation at high temperature, MCFC are susceptible to corrosion which reduces the cell life and overall efficiency. Carbonate produces Carbon dioxide which is very difficult to be separated from the generated water.

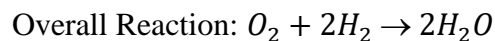
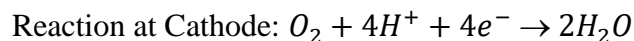
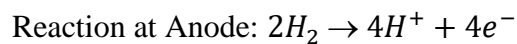
e. Polymer Electrolyte Fuel Cell

Polymer electrolyte fuel cells can be classified as i) Proton exchange membrane fuel cell (PEMFC) and ii) Anion exchange membrane fuel cell.

i) Proton exchange membrane fuel cells use a solid polymer electrolyte and precious metal (platinum) activated porous carbon electrodes. PEMFC are comparatively smaller in size and operate at low temperature (30-90°C), offering an advantage to start quickly and less wear and tear in the system. These fuel cells use pure hydrogen as a fuel and are very susceptible to carbon monoxide poisoning.

Water and heat management are the primary issues faced while operating a PEMFC. These type of fuel cells are generally used for transportation and stationary applications considering their remarkable power to weight ratio. The detailed construction and operation of PEMFC are discussed later in this report.

Reactions in PEMFC:



- ii) Anion exchange membrane fuel cells (AEMFC) are similar to proton exchange membrane fuel cells with a prime difference of alkaline membrane instead of acidic membrane used in PEMFC. In AEMFC, the  $\text{OH}^-$  ions are transported from cathode to anode instead of  $\text{H}^+$  ions transported other way round. Such reaction leads to alkaline pH in the fuel cells which offer certain advantages as improved oxygen catalysis and availability of variety of fuels including hydrogen.

Reactions in AEMFC:

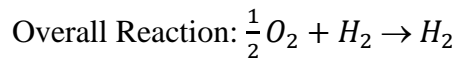
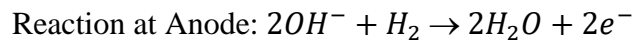
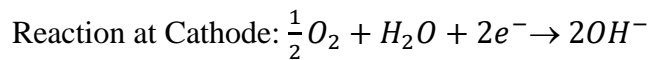


Table 1 Classification of Fuel cells. [1]

Type of Fuel cell	Operating Temperature (°C)	Advantages	Disadvantages	Applications
Alkaline Fuel Cell	60-250	High efficiency, Ease of heat and water management	Requires pure O <sub>2</sub>	Space
Phosphoric Acid Fuel Cell	160-220	CO tolerant, Waste heat durability	Low Power density, high cost	Stationary power
Solid Oxide Fuel Cell	600-1000	CO tolerant, can use various fuels, usable waste heat	Long startup time, require thermal shielding	Stationary power with cogeneration
Molten Carbonate Fuel Cell	600-800	CO tolerant, usable waste heat	Long startup time, electrolyte maintenance	Stationary power with cogeneration
Proton Exchange Fuel Cell	30-90	High efficiency, low wear, high power density	High cost, waste heat	Transportation and stationary power

## 1.2 Components of PEMFC

A PEMFC consists of four basic components.

- a. Solid polymer electrolyte membrane
- b. Catalyst layer
- c. Gas diffusion layer
- d. Bipolar plate.

These four components are used to breakdown protons and electrons from the fuel and transport species. The polymer electrolyte membrane conducts and transports the proton with the help of water and thus it is very important to regulate the heat and water in the

fuel cell. These components are assembled together as shown in Figure 1.1. At higher current densities, the water generated in the fuel cell prevents the diffusion of oxygen in the cathode catalyst layer resulting in increased mass transport overpotential of cathode which reduces the overall voltage of the cell. Hence, it is very important to manage the water balance in the system for efficient proton conductivity and efficient oxygen transport.

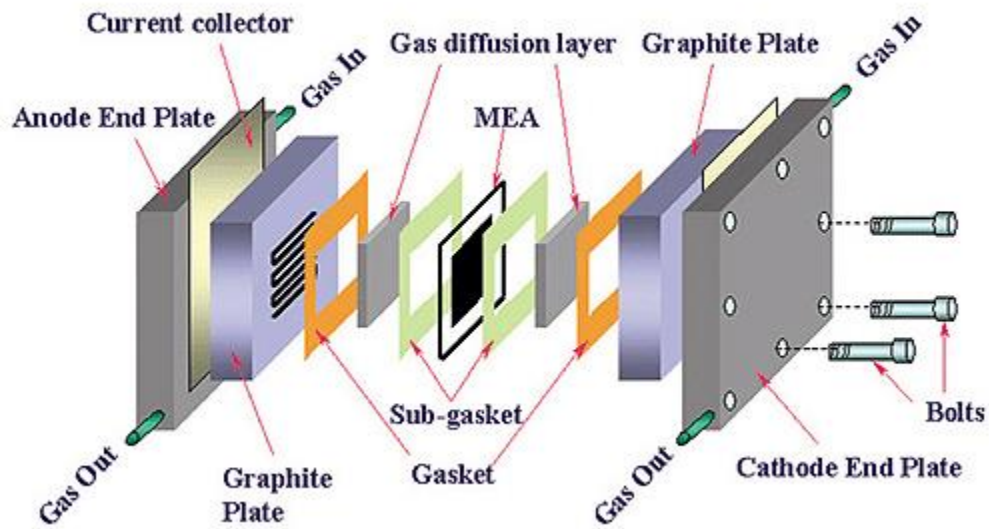


Figure 1.1. Schematic Representation of a PEMFC [2].

The importance and role of each of the component with respect to heat and water management, electron and proton transport is discussed below.

a. Polymer electrolyte membrane

Proton exchange membrane is one of the prime components of the PEMFC. It separates the reactants and allow only protons to pass by from anode to cathode. It also acts as barrier separating the anode and cathode gases as well as assuring no electronic conduction between the two electrodes resulting in higher power densities in PEMFC. The most common polymer electrolyte membrane is Nafion



(commercial product of DuPont) which is made up of perfluorosulfonic acid (PFSA) chain. This membrane needs to be hydrated adequately to transport the protons between the electrodes. Figure 1.2. shows the chemical structure of PFSA polymer chain in Nafion.

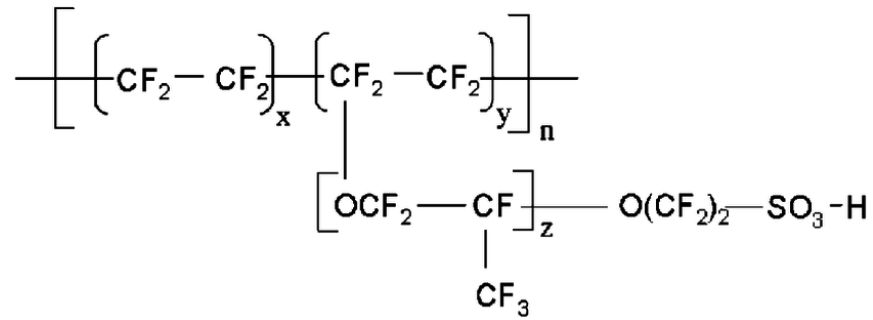


Figure 1.2. Chemical Structure of Nafion membrane

The desired proton conducting membrane should have following properties.

1. Excellent mechanical and electrochemical stability at the operating conditions.
2. Minimal resistive losses and no electronic conductivity to act as a barrier between two electrodes.
3. High proton conductivity to withstand high current densities.
4. Reactants should not be able to diffuse in the membrane to ensure high efficiencies.
5. Low cost and high operating life.

The proton conductivity of the membrane depends on the water content and the operation temperature of the fuel cell. There are two types of proton transport mechanisms based on the humidity of the membrane as explained by Weber et al. [3],[4]. At higher humidity, the proton transport mechanisms are non-classical such

as “Grotthus mechanism” where the proton is passed along with the hydrogen network present in the membrane. At lower humidity conditions, the proton is transferred using the surface mechanism with electrostatic diffusion provided by the sulfonate groups in the membrane. PFSA membrane provide all the required properties but are very delicate and costly due to its lengthy and critical chemical procedures.

b. Catalyst layer

Catalyst layers used at the anode and cathode of the PEMFC include platinum loaded carbon particles with a thin membrane of Nafion. The platinum acts as a catalyst whereas carbon particles provide the required mechanical strength and increased active surface area. The gases and protons get transferred through the catalyst layer and Nafion membrane by migration due to electric potential gradient whereas electrons are transferred to the reaction sites with the help of carbon particles.

Activation overpotential of anode is much less than that of cathode activation overpotential. This is due to the difficulty of catalyzing the oxygen reduction reaction. The catalyst at cathode is subjected to very corrosive environment and should be chemically stable to activate oxygen. The rate of hydrogen oxidation reaction (HOR) is very fast as compared to oxygen reduction reaction (ORR) due to the diffusivity of hydrogen in the catalyst layer and lesser number of electrons involved in the action.

Though platinum is an excellent catalyst to be used at anode for hydrogen oxidation reaction, it is very vulnerable to carbon monoxide (CO) poisoning. The anode is supplied with pure hydrogen gas but the traces of carbon monoxide is generally found due to manufacturing process involving reformation of hydrocarbons. CO consumes platinum by reacting and blocks the active area of the catalyst resulting in reduced reactivity.

Another problem faced at the cathode side is of flooding. The water produced at the time of operation in the cathode catalyst layer can block oxygen from diffusing in the catalyst layer which will result in overall voltage loss of the cell. This drawback can be tackled by increasing the amount of platinum loading on the cathode side which however will increase the cost of the PEMFC.

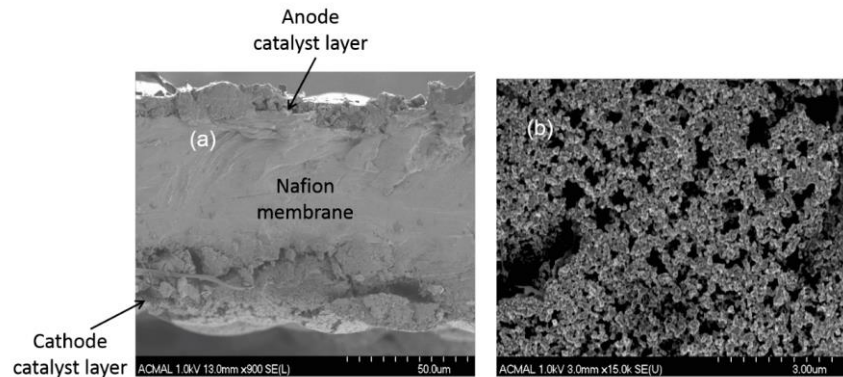


Figure 1.3. SEM images of catalyst coated membrane [5].

c. Gas diffusion layer

The gas diffusion layer (GDL) is assembled adjacent to the bipolar plates. It is made up of a porous carbon paper or a carbon cloth with very small thickness (100-300  $\mu\text{m}$ ). The main function of the GDL to diffuse the reactants to the catalyst layers

with minimum losses. It also provides the mechanical strength to catalyst layer increasing the active surface area and conducts electrical current as well as provides pathways for water to move from the reaction site to the flow channels.

The structural, thermal, electrical as well as chemical properties of the GDL plays an important role in the operation of a PEMFC. Properties such as electrical conductivity, thermal conductivity, porosity, pore distribution ratio is very important for the electron transport, mass fuel transport, water and thermal management in the PEMFC.

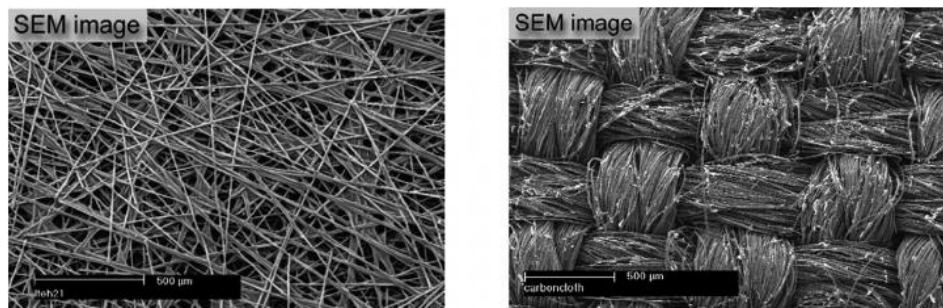


Figure 1.4. SEM image of Toray 060 carbon paper (left) and E-Tek carbon cloth [5].

#### d. Bipolar plates

Bipolar plate is another important component of the PEMFC. The bipolar plates are responsible to transport the hydrogen and oxygen to the catalyst layers and remove the heat and water generated from the catalyst layers. It also transports electrons and provide the structural support (80% of the weight) to the entire fuel cell assembly. The bipolar plate consist of flow channels of which flow field design plays a vital role in the performance. There are various types of flow field designs such as straight, serpentine, interdigitated, etc. with which they provide different flow patterns such as co-flow, counter flow or cross flow.

## 2 Operation Principle of PEMFC

The proton exchange membrane fuel cell is one of the most promising fuel cell technologies. In a PEMFC, pressurized hydrogen gas is supplied to the anode side. This gas is further diffused in the anode catalyst layer where it encounters platinum (catalyst). On reaction with platinum, the hydrogen molecule is split into  $H^+$  ions and electrons. The  $H^+$  ions are further passed through the proton exchange membrane to the cathode side whereas the electrons are passed through the external circuit generating current. Simultaneously, at the cathode side, oxygen is supplied and is diffused through the cathode catalyst layer. The supplied oxygen reacts with hydrogen ions to generate water consuming electrons from the external circuit. Figure 2.1 shows the working principle of a PEMFC.

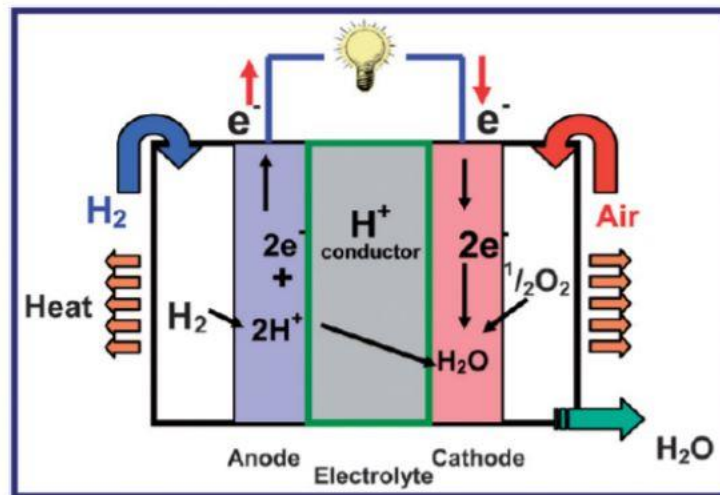


Figure 2.1 Working principle of PEMFC [6].

## 2.1 Performance of PEMFC

The characteristic study of the performance of the fuel cell can be done by analyzing the polarization curve (voltage vs current density) as shown in Figure 2.2. Based on the factors that affect the performance of the fuel cell, a polarization curve can be divided into five regions.

1. Activation polarization region
2. Ohmic polarization region
3. Concentration polarization region
4. Hydrogen crossover region
5. Thermodynamic region

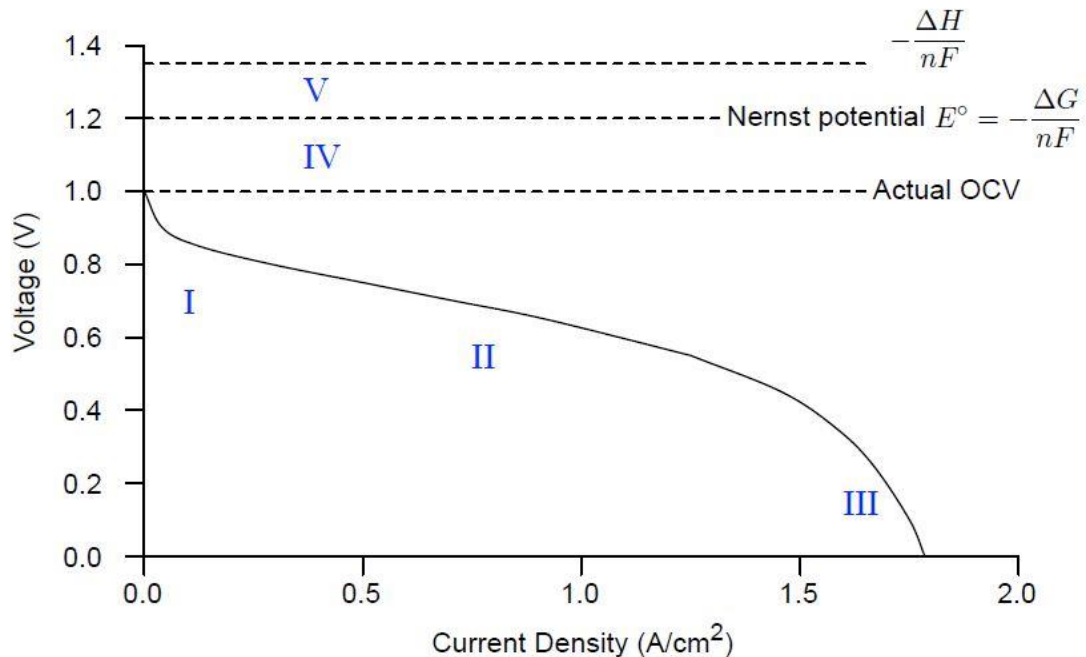


Figure 2.2. Sample polarization curve of PEMFC

## 1. Activation polarization Region

In the low current density regions, when the current is drawn, voltage loss is observed from the equilibrium value. This voltage loss is due to the activation energy required to initiate the redox reactions at both the electrodes. This loss is also known as activation overpotential.

This activation overpotential can be calculated using a Butler-Volmer equation as follows.

$$i_{cell} = i_0 \left[ \exp\left(\frac{\alpha_a F}{RT} \eta\right) - \exp\left(\frac{-\alpha_c F}{RT} \eta\right) \right]$$

Where,  $i_{cell}$  is the current density generated by the cell (A/cm<sup>2</sup>),  $i_0$  is exchange current density (A/cm<sup>2</sup>),  $\alpha_a$  and  $\alpha_c$  are anodic and cathodic charge transfer coefficients respective, R is universal gas constant (J/mol), T is cell temperature (K), F is Faraday's constant (C/mol) and  $\eta$  is activation overpotential.

## 2. Ohmic polarization region

The voltage loss in the ohmic polarization region is due to the resistance to charged species transport such as electron transport resistance or ion transport resistance.

This voltage loss is known as ohmic overpotential. To represent the resistance of every component, area specific resistance 'r' ( $\Omega \cdot \text{cm}^2$ ) is used.

Ohmic overpotential can be calculated using Ohm's law as follows.

$$\eta = i_{cell} * \sum r$$

where,  $i_{cell}$  is the current density generated by the cell ( $A/cm^2$ ),  $\sum r$  is the summation of area specific resistance of all the components that have electron or ionic transport resistance ( $\Omega \cdot cm^2$ ) and  $\eta$  is ohmic overpotential.

### 3. Concentration polarization region

In the high current density region, the voltage loss caused due to the inadequate mass transport to and from the reaction site is known as concentration overpotential. This is due to the high rate of the reaction but slow rate of mass transfer to the catalyst. Due to this slow rate, the reactants can't reach, and the generated products can't leave from the catalyst. As the cell is subjected to high current density, the reactants are consumed, and products are accumulated at the electrode surface which increasingly causes more obstruction to the reactant flow.

### 4. Hydrogen crossover region

The primary and most important component of the fuel cell assembly is the electrolyte membrane. This membrane is responsible to transport ions from one electrode to another and physically fence the fuel and the oxidizer to avoid the direct reaction. However, these membranes are not perfectly efficient as some of the gases permeate through the membrane due to the pressure as well as concentration gradient between the two electrodes. This phenomenon is known as gas crossover. The voltage loss in this region is due to the molecular diffusion of hydrogen through the membrane. This hydrogen reacts directly with the oxygen which decreases the electrochemical potential. This loss can be calculated as follows.

$$i_{cross} = -i_0 \exp\left(\frac{\alpha_c F}{RT} \eta\right)$$



Where,  $i_{cross}$  is equivalent current density due to gas crossover and  $\eta$  is crossover overpotential.

### 3 Segmentation of PEMFC

The reactant and water distribution are the primary parameters affecting the performance of a PEMFC. To study these mechanisms within a component of the cell as well as between the connecting interfaces of the two components, local or individual evaluation is must. Segmented PEMFC is one of the local diagnostic method used to evaluate the local current densities, ohmic resistance, electrochemical active area, etc. These local measurements can be used to evaluate the factors that affect the local voltage losses. The design of cell affects the consumption rate of the fuel which leads to local water production, generating non-uniform local current densities and ohmic resistances which are different from the overall reading of the cell.

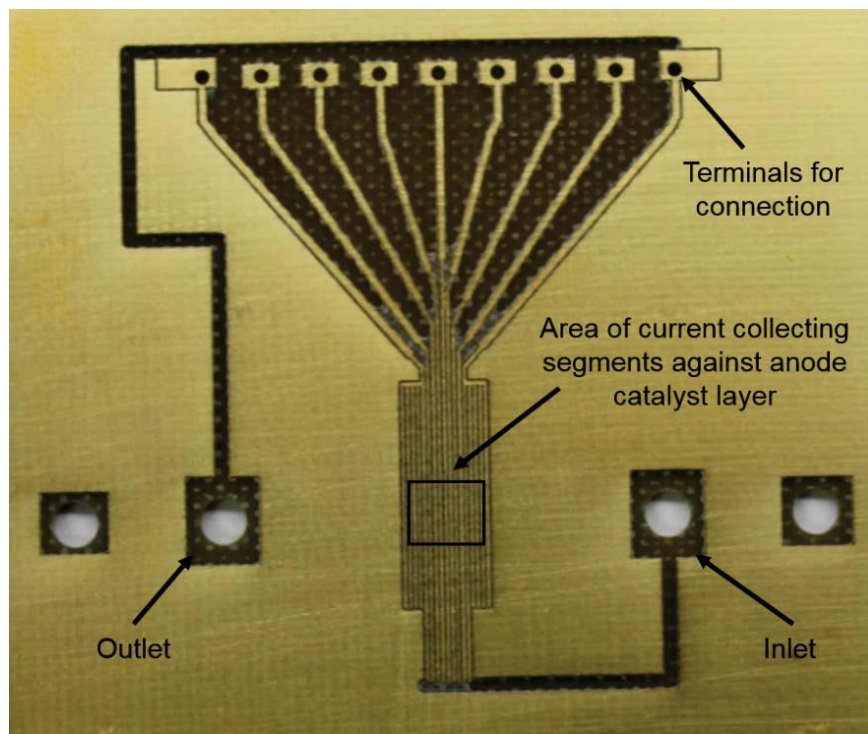


Figure 3.1. Segmented current collector

The segmented flow field allows to analyze the local transport mechanism and the effect of local water generation on overall cell performance. Figure 3.1 shows a segmented flow current collector design used to measure local current density and ohmic resistance distribution along the land channel geometry of the cell. The 9 segments provided on the collector allows hydrogen to flow through 8 channels present between the consecutive two segments. The current produced in the local area due to the local electrochemical interaction of the reactants allows us to study the transport mechanism and overall effect on the cell performance.

There are various techniques developed for the measurement of local current density distribution. Cleghorn et al. [7-10] developed a printed circuit board (PCB) approach to measure the local current distribution. This technique was used along with segmented electrodes and was proved useful for various reactant flow and humidification strategies. In this method to measure a local current distribution in the individual segments, each segment was decoupled from the rest of the segments on the PCB and the current and voltage sense of the selected segment was connected to the external load box which allowed them to measure the current distribution of each and every segment and study its effect on the overall performance of the cell. Geiger et al. [11] came up with a novel technique including magnetic loop array with closed loop Hall effect sensors to monitor the current distribution. In this method, a current sensor is used to measure the current in the individual segment. This Hall effect sensors generates a magnetic field with respect to the primary current and gives out the voltage of the hall generator which is in proportion with the primary current. With the help of boosted circuit an opposing magnetic field is

generated to drive the core to zero flux. This opposing magnetic field produces the secondary current which can be measured with the help of accurate resistor. Stumper et al. [12] used a sub-cell partial electrode membrane assembly to measure the current distribution.

Segmented fuel cell technique is used in various research to evaluate the effect of local parameters on the fuel cell performance. Hakenjos et al. [13] implemented a segmented anode approach to evaluate the local water flow distribution and its effect on the current density for various air flow rates. Similarly, Sun et al. [14] used a segmented fuel cell method to evaluate the effect of operating temperature, fuel flow rate and relative humidity on the local current distribution of the cell. Dong et al. [15] designed a segmented cathode flow field to evaluate the local ohmic resistance and current density distribution to study the effect of cathode humidification on the water distribution in the cell.

## 4 Importance of Land Channel Geometry: Literature Review

The flow field geometry of a PEMFC is made up of a land and channel as shown in Figure 4.1. The purpose of the land is transporting the electron and remove heat from the system and channel ensures the flow of reactants and products to and from the reaction site. The following literature survey serves the purpose of understanding the effect of the land channel geometry on the performance parameters of the fuel cell.

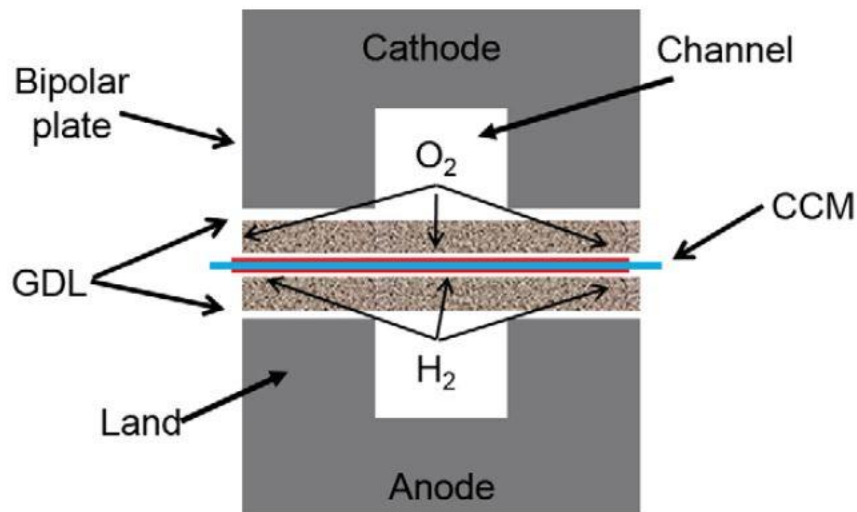


Figure 4.1. Schematic diagram of land channel geometry in the flow field of a PEMFC [16]

Due to the complexity of fabricating such a small-scale assembly and difficult of making electrical connection in very small available area, researchers use a very complex models, imaging techniques and ex-situ experiments to study the transport phenomena in the land channel direction of the fuel cell.

## 4.1 Effect on Water Distribution

In the high relative humidity setup, the land channel geometry is responsible for the non-uniform water distribution in the GDL. This non-uniform distribution can be the primary reason disoriented current generation and thus it is necessary to study species distribution in the land channel direction. Wang et al. [17] developed a numerical model to analyze the water distribution in the land channel direction and concluded that at higher current density regions, the water accumulated under the land region is four to five times as that of the channel region. Figure 4.2 shows their findings for 100 % relative humidity.

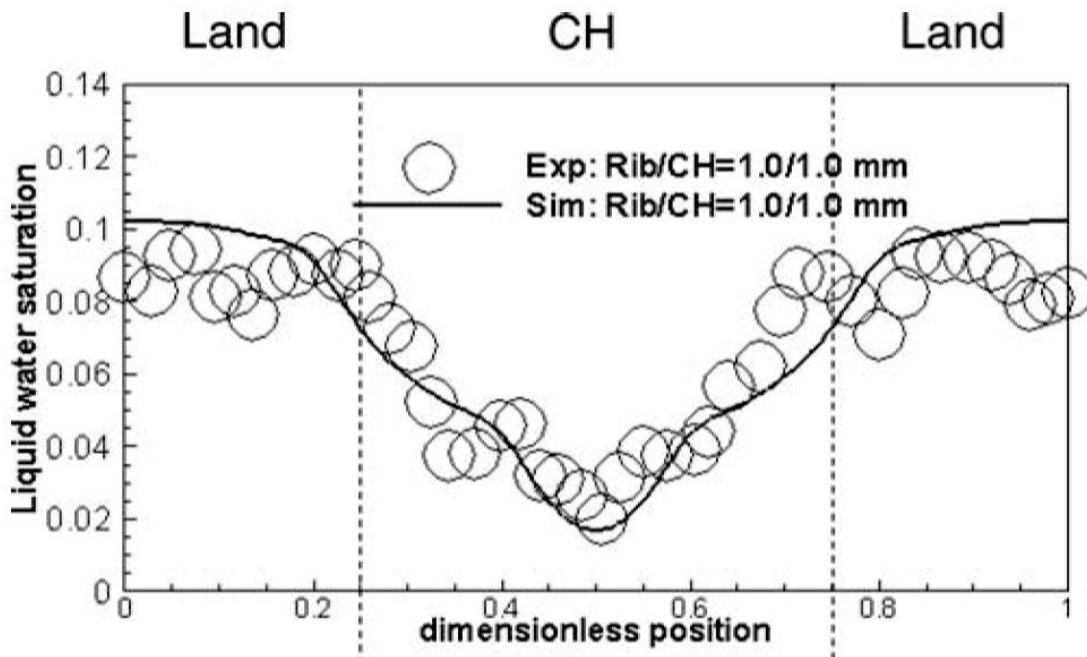


Figure 4.2. Water distribution in GDL with respect to land channel geometry at 80°C and 2.5 A/cm<sup>2</sup> current density.

Further, Deevanhaxy et al. [18] and Eller et al. [19] used X-ray radiography and X-ray tomography techniques respectively for imaging the water saturation in the land channel

direction. Results of both lead to the higher water saturation under the land channel exists and can cause mass transport resistance decreasing the overall efficiency of the cell. Similarly, Natarajan et al. [20] also found out the heavy water accumulation under the land channel in the low current density region and concluded the non-uniform water distribution has a greater impact on the reactant low resistance as well as the electron transport resistance. Considering all the results mentioned above, it is necessary to study the local current density distribution to understand the effect of water accumulation on the overall current density of the fuel cell.

## 4.2 Effect on Current Distribution

The land channel geometry leads to uneven transport pathways, non-uniform water accumulation in the GDL as well as in the membrane, varying electrical and transport resistances leads non-uniform reactant flow which generates uneven local current densities in-plane direction of PEMFC. This study of these uneven pattern of local current generation can help understand the transport phenomenon in the fuel cell.

Researchers have tried various numerical as well as experimental approaches to analyze this pattern and understand the overall impact of the flow field geometry on the cell performance. For the interdigitated flow field, He et al. [21] found out that the local current density for the channel region closer to inlet has a higher current density and further goes on decreasing as we move forward in the outlet region direction. Figure 4.3 demonstrates his results for the local current density distribution.

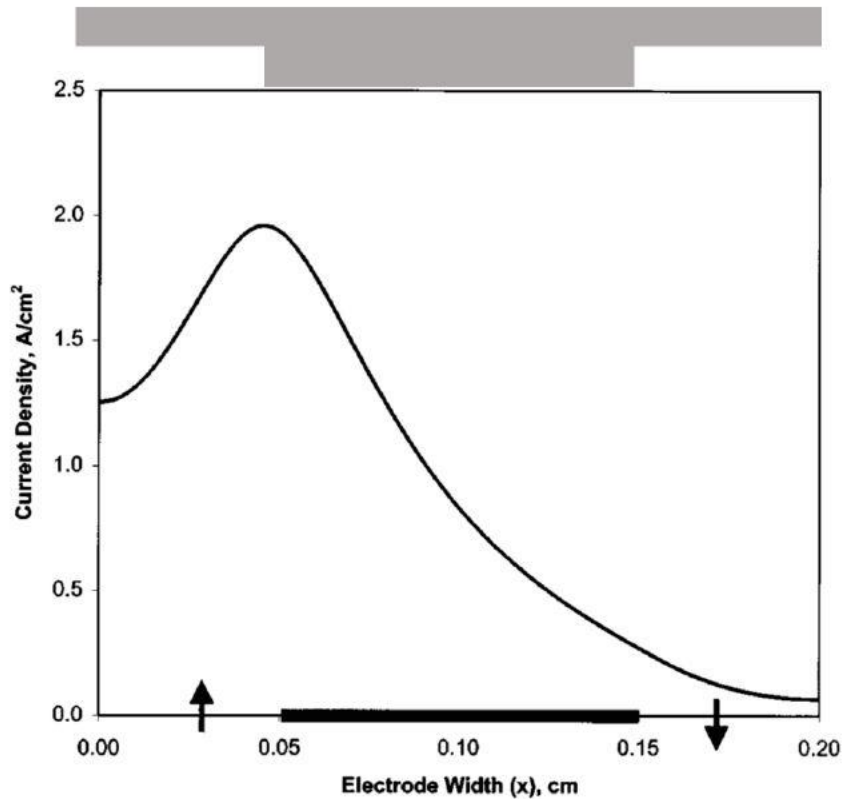


Figure 4.3. Current density distribution for interdigitated flow pattern

Further, Meng et al. [22] studied the current density distribution with respect to the water content in the GDL for high humidity setup. He compared heavily flooded GDL and very dry GDL to analyze the distribution for the same setup. In conclusion of his simulation he found out that the difference between the land and channel current generation is comparatively low as in the case of flooded GDL setup. He believes the higher transport resistance in the case of flooded GDL led to these results. Figure 4.4 shows the results for his experiments.



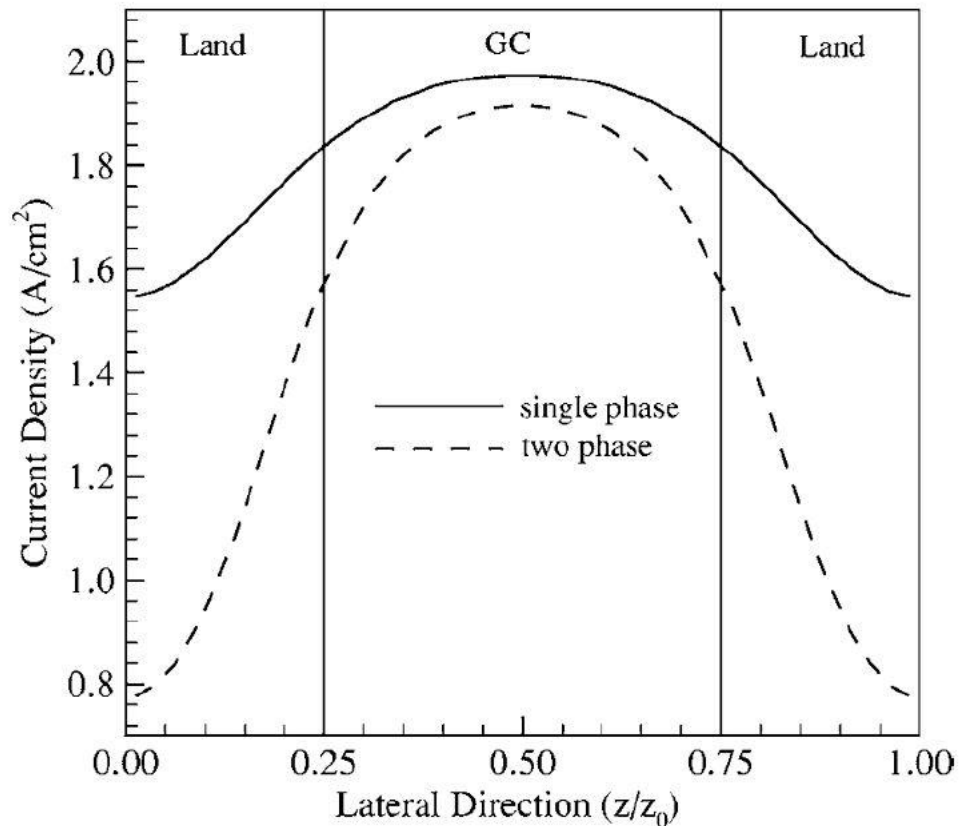


Figure 4.4. Local current density distribution for dry and flooded GDL setup at 80°C.

Freunberger et al. [23] applied an experimental approach to study the local current density distribution using segmented cell approach. He used gold plated probes place at the junction of the two interfaces to measure the potential difference between the two components. According to his findings, in the higher global current density region, the current density under the channel region is higher than the current density under the land region. For the lower global current density region, he found out the exact opposite results where current density under the land channel was higher than the channel region. The inadequate hydration of the membrane leads to these results.

## 5 Experimental Setup

### 5.1 Design of Segmented Anode Flow Channel [16]

A new approach was considered to manufacture the segmented cell in which the anode current collector plate is segmented, and cathode current collector plate has a single land channel geometry. This design can be used according to the flow design such as cross flow, counter flow, etc.

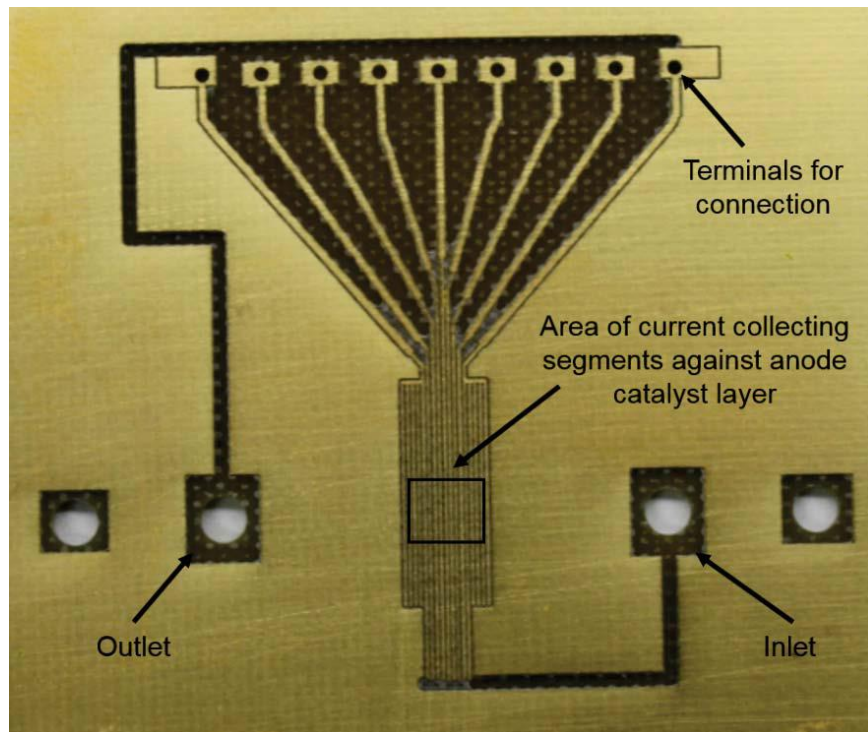


Figure 5.1. Segmented anode side current collector

In this design, multiple flow channels for the hydrogen transport were created. As show in Figure 5.1, this anode current collector consists of nine lands and 8 channels. The land width being  $200\ \mu\text{m}$  and is made up of gold-plated copper to avoid the corrosion. The  $150\ \mu\text{m}$  separation between the two land segments are used as flow channels for the hydrogen

flow. The dimension of the catalyst layer was kept to be 3 mm x 3 mm active area resulting in approximately a spatial resolution of 350  $\mu\text{m}$ .

The high amount of platinum loading was used on used on the anode catalyst for the faster rate of hydrogen oxidation and GDL from the anode side was removed to avoid in-plane current generation. Eliminating anode GDL resulted in high in-plane resistance which can be used for the accurate local current density measurement. On the cathode side, a single land channel geometry of 1 mm configuration was used without any segmentation.

## 5.2 Design of Current Distribution Measurement System [16]

In this experimental approach, a high frequency resistance (HFR) method is used. In this method, an alternating current is supplied to the segmented cell and the voltage drop across the cell is measured. Further, using Ohm's law, the high frequency resistance of the cell can be calculated.

For the measurement of the local current density, a PCB design approach was selected as shown in Figure 5.2. Nine shunt resistors of 200 m $\Omega$  were connected in a parallel fashion representing the electronic and protonic resistances of the cell in the in-plane direction of the PEMFC. Using a high-resolution multimeter, (Keithley Instruments DMMA 2700), we can calculate the voltage drop across each of the shunt resistor and the local current for each of the segment can be calculated using Ohm's law as follows.

$$I_{AC}^n = \frac{V_{AC}^n}{R_s}$$

Where,  $R_s$  is the shunt resistance and  $n$  is the selected segment number.

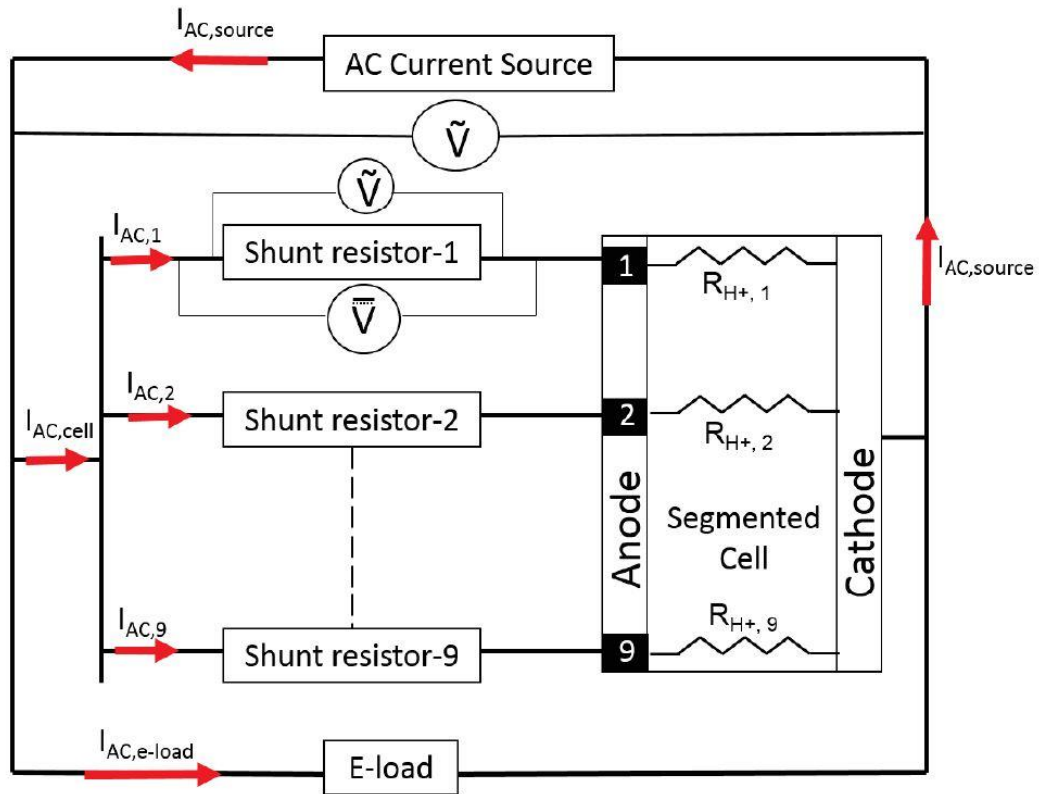


Figure 5.2. Experimental setup for measurement of local current density

### 5.3 Preparation of Membrane Electrode Assembly (MEA)

A catalyst coated membrane of  $0.4 \text{ mg/cm}^2$  of platinum loading consisting of platinum catalyst (40% of Pt/Vulcan C) and Nafion ionomer solution (D2020) with ionomer/carbon weight ratio of 0.8 was supplied from the facility of University of Calgary, Alberta, Canada. To prepare the membrane electrode assembly, a small window of  $3 \text{ mm} \times 3 \text{ mm}$  and  $4 \text{ mm} \times 4 \text{ mm}$  was cut out from two individual Kapton sub-gaskets using Silhouette Cameo precision cutter. Further, a Nafion membrane (NRE 212) was pressed between the two sub-gaskets. The catalyst layer was punched out from the respective anode and cathode

sheets of catalyst inks and was placed in each of the cut-out windows on the Kapton sub-gaskets as shown in Figure 5.3.

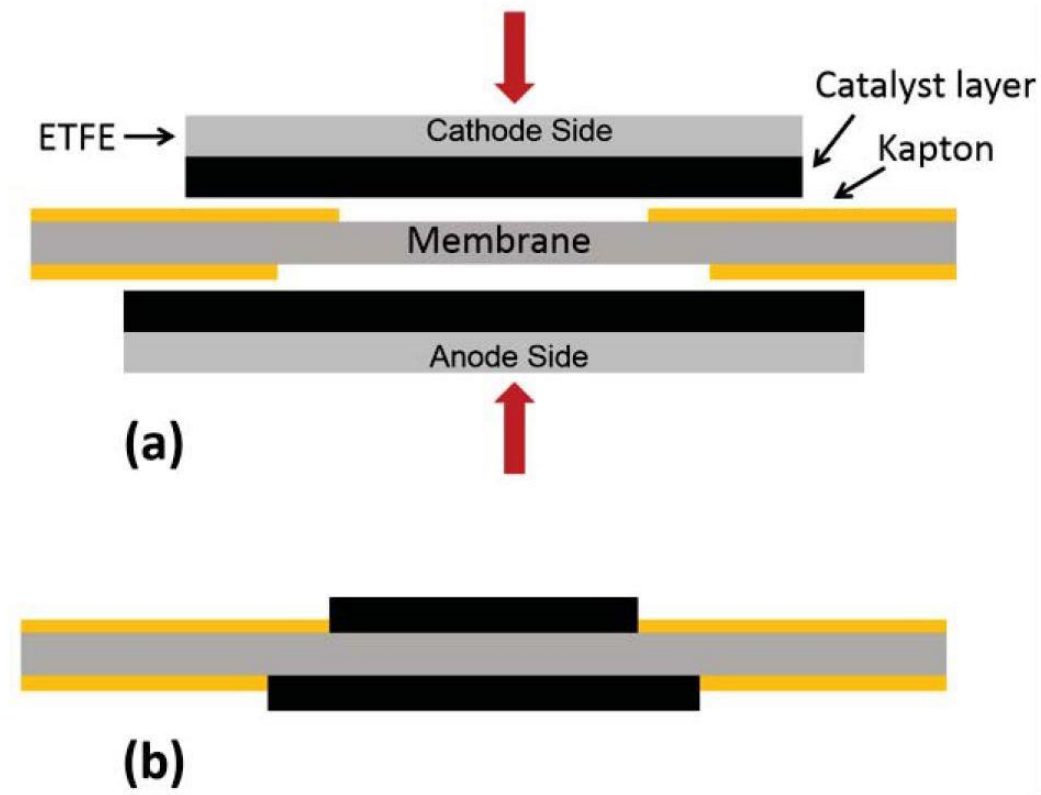


Figure 5.3. Schematic representation of MEA preparation a) Catalyst coated membrane sandwiched between anode and cathode assembly b) cross section of MEA

Then this subassembly was placed between two cardboard sheets for uniform pressure distribution and was put on the hot press. The catalyst was transferred on the Nafion membrane (NRE 212) by hot pressing the subassembly at 150°C and 2.75 MPa pressure for 3 minutes as shown in Figure 5.4.

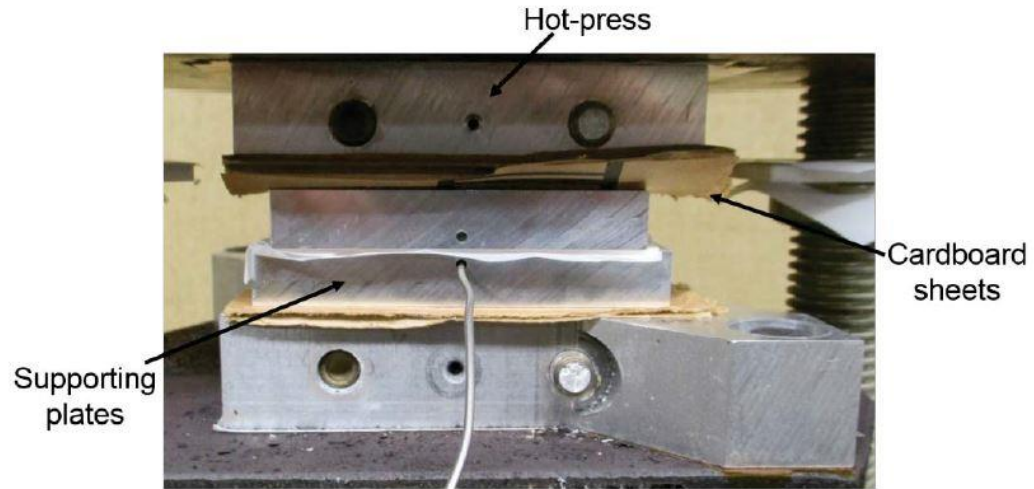


Figure 5.4. Catalyst coated membrane in the hot press.

#### 5.4 Assembly of Segmented Cell

For the assembly of the cell, graphite bipolar plates were used at both anode and cathode. A carbon paper (TGP-H-90) was used as a GDL on the cathode side with a dimension of 5 mm x 5 mm. A 250  $\mu\text{m}$  PTFE was used to seal the GDL in the assembly to achieve 20% compression. The schematic diagram of the cell assembly is shown in the Figure 5.5.

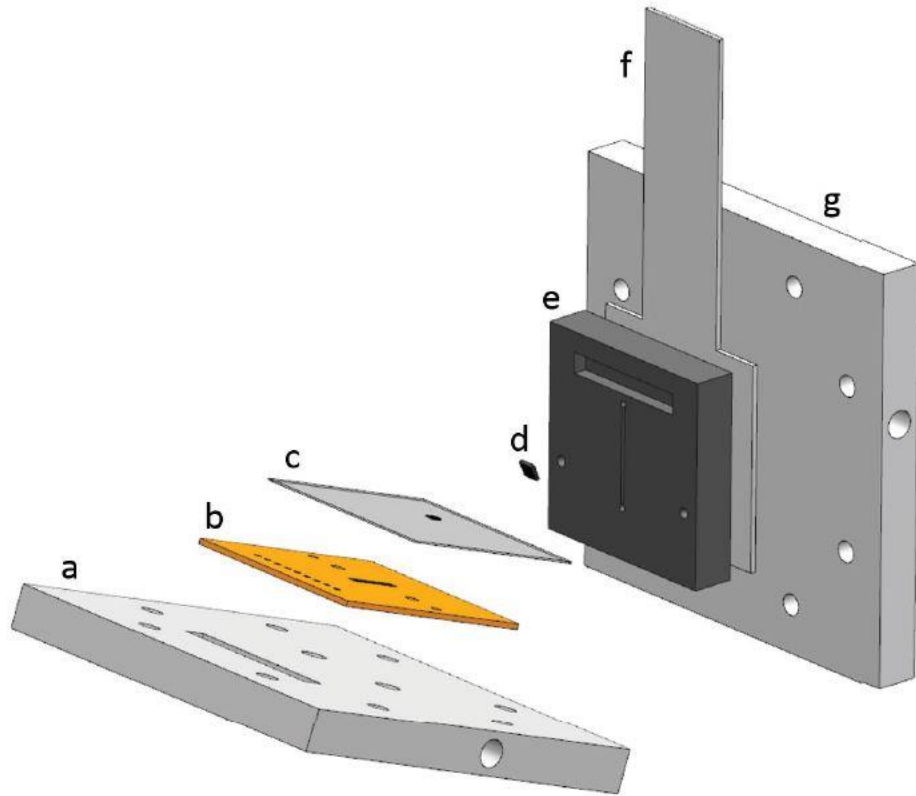


Figure 5.5. Assembly of segmented cell representing a) Anode end plate b) Segmented anode current collector c) Catalyst coated membrane d) Cathode GDL e) Cathode bipolar plate f) Cathode current collector g) Cathode end plate [24]

Further the catalyst coated membrane was fused in between the cathode side assembly and segmented anode side assembly with the compression pressure of 2 MPa to ensure proper sealing and avoid any leakage and damage to any component. Figure 5.6 shows the anode and cathode assembly and Figure 5.7 shows the cross section of the segmented cell assembly.



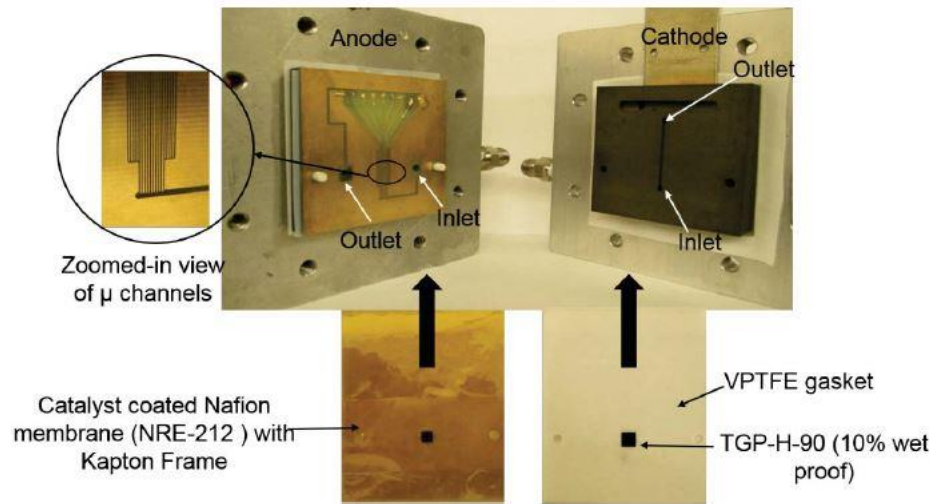


Figure 5.6. Components of Segmented cell assembly

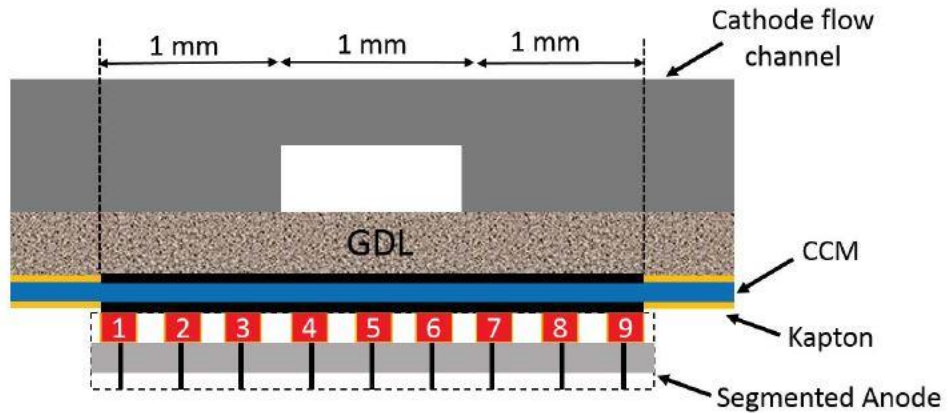


Figure 5.7. Cross section view of segmented cell assembly [16]

On completion of segmented cell assembly, preconditioning was performed based on the New Energy and Industrial Technology Development Organization (NEDO), Japan suggested parameters as mention in Table 2. For the control of relative humidity, pressure, cell temperature and mass flow rates of the reactants Fuel Cell Technologies' test stand was used. For the control of supplied Voltage and Current, a Vertex potentiostat from



Ivium technologies was used. For the measurement of local current generation, Keithley digital multimeter was used. Once the precondition of the fuel cell was performed, the testing was conducted as mentioned in Table 3.

Table 2. NEDO preconditioning parameters for PEMFC

Parameter	Value
Area of cell	9 mm <sup>2</sup>
H <sub>2</sub> flow rate	70 sccm
Air flow rate	100 sccm
Cell temperature	80°C
Anode relative humidity	88 %
Cathode relative humidity	42 %
Duration	6 hours

Table 3. Testing Conditions for the measurement of the local current density in the land channel direction.

Control Type	Pressure (psi)	Cell Temperature (°C)	An/Ca Relative humidity (%)	An/Ca flowrates (sccm)	An/Ca Fuel
Voltage	5	60	80/80	70/70	H <sub>2</sub> /Air
Voltage	5	60	80/60	70/70	H <sub>2</sub> /Air
Voltage	5	60	50/0	70/70	H <sub>2</sub> /Air

## 6 Results and Discussions

According to the test conditions mentioned in Table 3, the segmented PEMFC performance was analyzed to understand the effect of relative humidity (RH) considering the local current distribution in the land channel direction. The cell was operated with hydrogen as an anode gas and air supplied to the cathode. Figure 6.1 shows that the overall cell performance is affected by the humidity content as the overall ohmic resistance and oxygen transport resistance tend to increase.

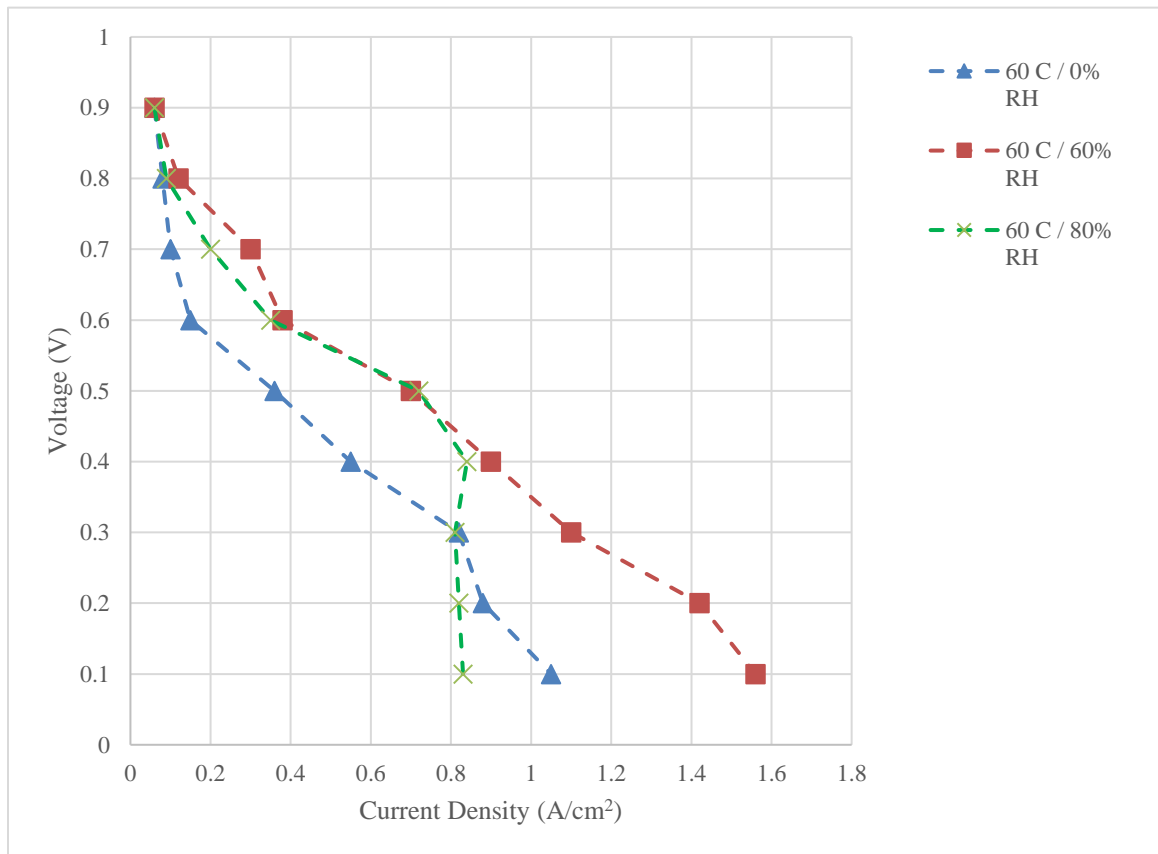


Figure 6.1. Performance of cell at dry, moderate and wet humidity conditions

In dry condition (0% RH), the limiting current density is observed to be around 1 A/cm<sup>2</sup>.

This value is comparatively low as compared to regular fuel cell performance. In dry

condition, this lower limiting current density is the effect of higher proton transport resistance as well as the catalyst layer dehydration. As mentioned earlier in this report, catalyst layer requires adequate amount of water to transport the ions from one electrode to another, which in this case is very low. Thus, catalyst layer has to be dependent solely on the current generation which generates water.

In wet condition (80% RH), the limiting current density of the cell is approximately 0.8 A/cm<sup>2</sup>. In this case, at the limiting current density value, severe flooding is observed due to the over-hydration of the membrane. This is due to higher humidity condition and current generation which hinders the oxygen transport to the cathode catalyst layer. This hinderance increases the concentration overpotential in the cell and a sudden voltage drop is observed.

In the moderate humidity setting (60% RH), the proton and oxygen transport resistances are very much critical at low to moderate current density regions. With increased current generation, water production due to the redox reaction increases and hydrates the membrane, resulting in decrease of the overall concentration or mass transport overpotential significantly. Thus, we can observe that the limiting current density for moderate humidity condition is approximately 1.6 A/cm<sup>2</sup> which is much higher than the previous two conditions.

Further, the analysis of local current distribution is performed for the same conditions as presented in Table 3. In the following figures and analysis, segments 1, 2, 8 and 9 represent the land while segments 3, 4, 5, 6 and 7 represent the channel region.

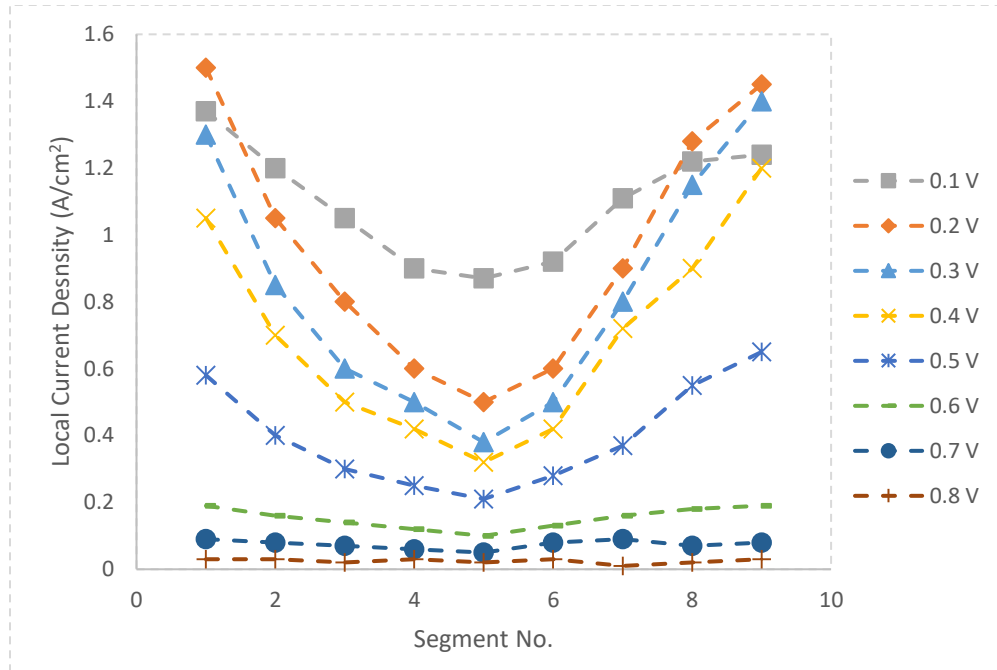


Figure 6.2. Local current distribution for dry condition

As observed in Figure 6.2, in dry condition (0% RH), at all the cell voltage the local current density generated in the channel area is much lower than that of current density generated in the land region. At 0.2 V, the current density generated in the center segment of the channel region is 0.6 A/cm<sup>2</sup> while for the same cell potential the current density at the extremes of the land channel (segment 1 and 9) is 1.4 A/cm<sup>2</sup>. In the dry setting, the dehydrated membrane and catalyst layer is the primary reason for the voltage loss and thus, the local current generation is totally driven by the local ohmic resistance of the segment. Paul et al. [25] also concluded that in dry condition the proton conductivity thin membrane is much lower than that of thick membrane.

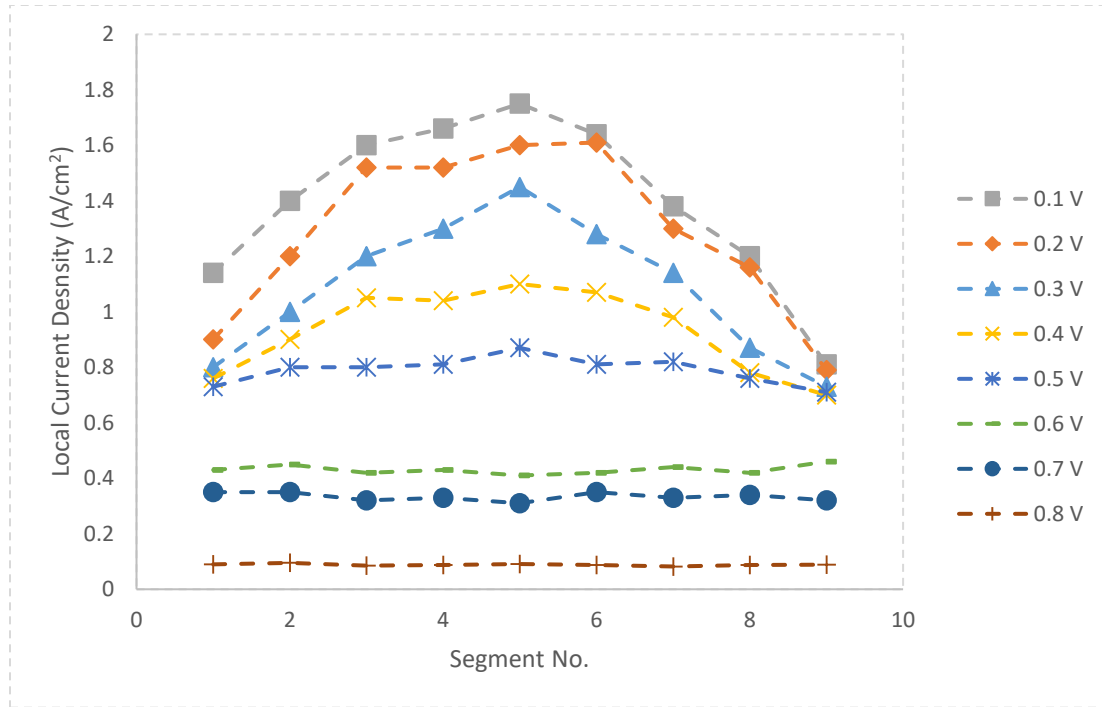


Figure 6.3. Local current distribution in wet condition

In wet condition (80% RH), the trend of local current distribution is observed to be exactly opposite to the trend in dry condition. The current generation in the channel is significantly higher than the land region. At 0.3 V, the maximum current density at the center of the land region is  $1.39 \text{ A/cm}^2$  whereas at the extremes of land channel it is found to be  $0.8 \text{ A/cm}^2$  for the same cell potential. As seen in the Figure 6.3, the local current density distribution under the channel start to drop considerably after 0.6 V of cell voltage. This sudden drop in the cell potential indicates huge amount of water accumulation under the channel region. The current generation under the channel region being the prime factor of overall cell current density, the accumulation or flooding of the water under the channel region decreases the overall performance of the cell.

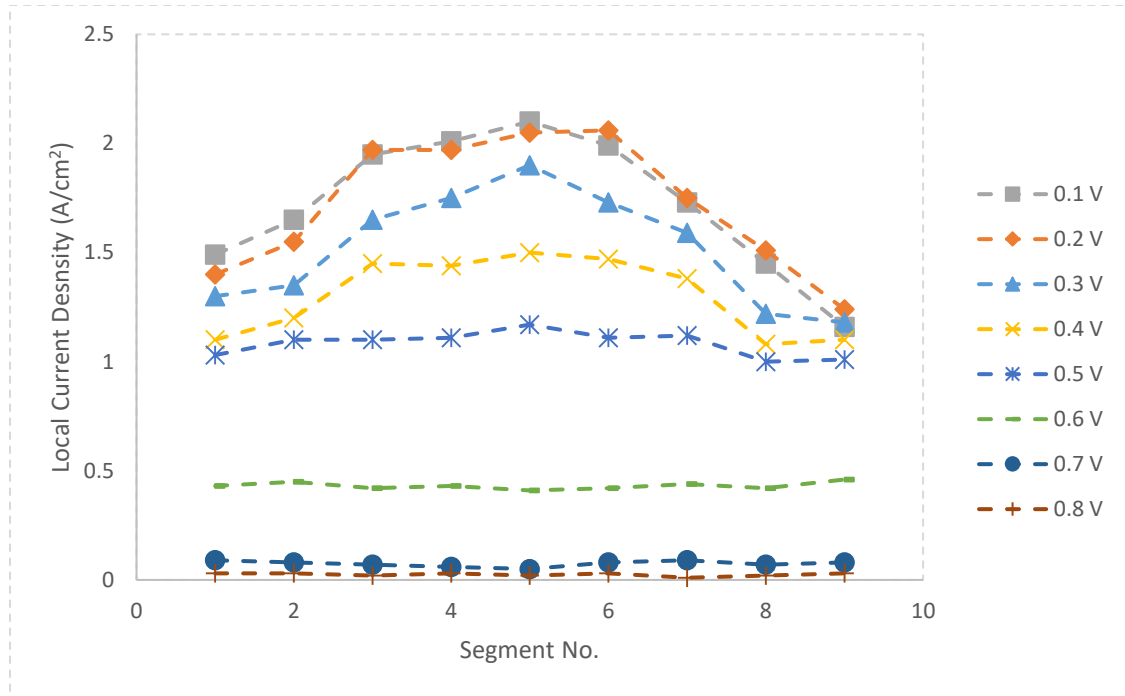


Figure 6.4. Local current density distribution in moderate humidity setup

For the moderate humidity conditions (60% RH), the local current distribution is uniform under both land and channel region for the cell potential above 0.3 V while overall current density being lower than 1.4 A/cm<sup>2</sup>. For example, at 0.5 V, the current density in the land region is 1 A/cm<sup>2</sup> while at the center of the channel region is 1.06 A/cm<sup>2</sup> which is approximately uniform. When the cell voltage decreases under 0.3 V, we can observe an uneven trend of local current distribution. The current generation under the land area is lower than that of current generation at the center of channel region. For example, at 0.1 V cell potential, the current density at the extremes of the land is 1.5 A/cm<sup>2</sup> and at the center of the channel is 2 A/cm<sup>2</sup>. The trend at this cell potential closely aligns with the trend of current distribution in the wet condition. Considering the comparison, the uneven current distribution profile depict that the cell is moving into wet condition. This transition in the

wet phase is due to the increased rate of water production associated with the higher local current densities.

For the moderate humidity condition, performance of each segment was analyzed and plotted as shown in Figure 6.5.

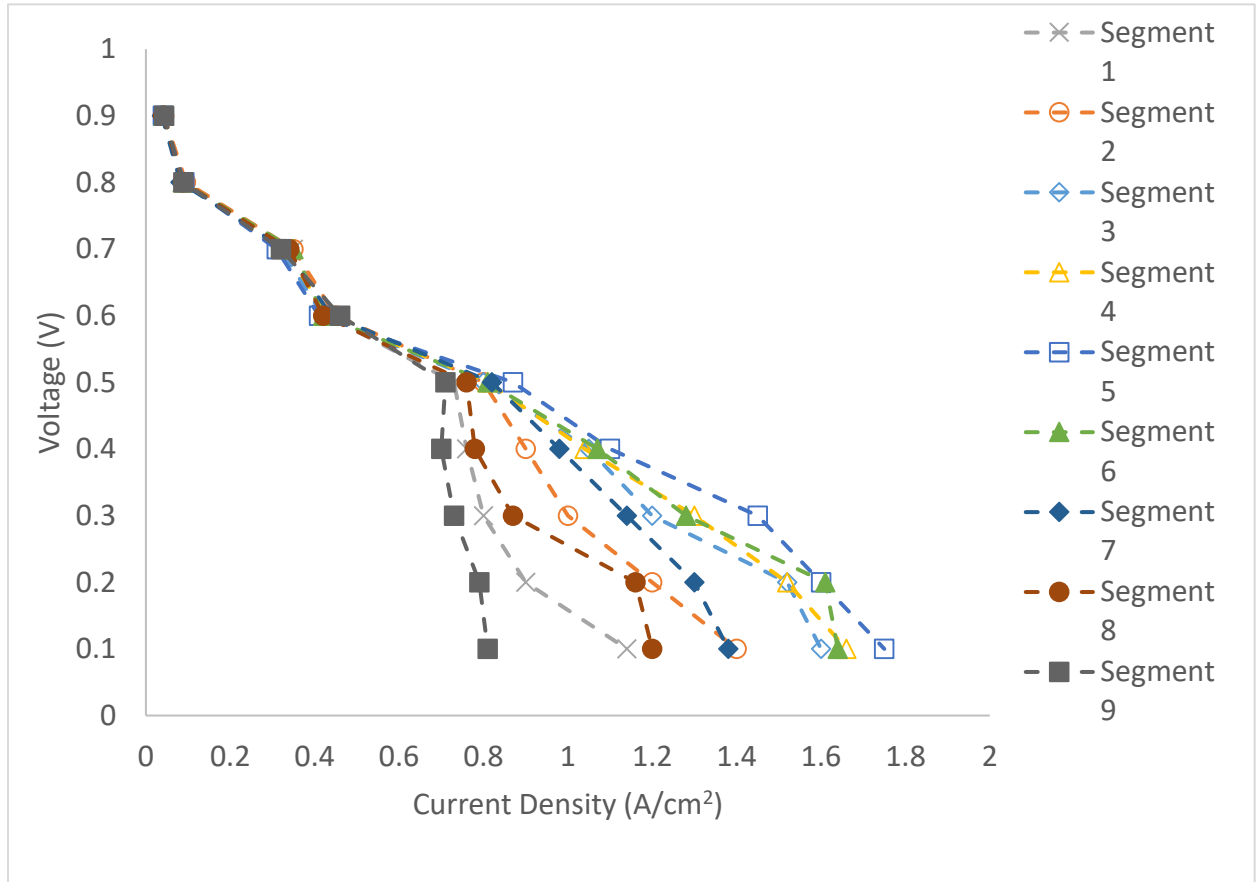


Figure 6.5. Performance of individual segment for moderate humidity condition

If we observe the limiting current densities for the segment under the end tip of the land region (segment 1, 9) and at the center of the channel region (segment 5), it increases from 0.8 A/cm<sup>2</sup> to 1.8 A/cm<sup>2</sup>. As the cell potential starts dropping below 0.4 V, we can notice that the current generation in the land region starts to extremely decrease due to the water

generation. From this plot, we can conclude that the water accumulation under the land region is higher as the distance between the catalyst layer and channel is comparatively larger in the land region and hence affects the amount of oxygen diffusion in the catalyst layer under this region.



## 7 Conclusions and Future Work

In this experiment, a highly precise segmented with an active area of  $9 \text{ mm}^2$  with a  $350 \text{ }\mu\text{m}$  resolution was designed and fabricated. On in-house manufacturing of catalyst coated membrane, using cathode single land-channel geometry bipolar plate and segmented anode current collector the cell was assembled. Further, the cell was conditioned based on NEDO suggested parameters. A novel PCB approach was used for the data acquisition of the local current distribution was used.

In wet condition, the current distribution in the land region was much lower than that of the local current generation in the channel region. Uneven water distribution and accumulation was the primary source for lower limiting current density. On the other hand, in dry condition, the current distribution under the land his effectively higher than in the channel region. The dehydration of the membrane governs the performance losses in this condition resulting in increased concentration overpotential. In moderate humidity conditions, at higher cell potential uniform current distribution is observed. As the cell voltage goes below  $0.3 \text{ V}$ , the transition in the wet phase causes water accumulation under the land region resulting in uneven current distribution in this setup.

In future, this segmented cell can be used to understand the effect of oxygen transport on overall cell performance as well as to evaluate the ionic resistance distribution of the catalyst in the land channel direction for various flow field designs.

## 8 References

1. Mench, M.M., *Fuel cell engines*. 2008: John Wiley & Sons.
2. Al Lafi, A.G., *Cross linked sulphonated poly (ether ether ketone) for the development of polymer electrolyte membrane fuel cell*. 2009, University of Birmingham.
3. Weber, A.Z. and J. Newman, *Transport in polymer-electrolyte membranes II. mathematical model*. 2004. **151**(2): p. A311-A325.
4. Weber, A.Z. and J. Newman, *Transport in polymer-electrolyte membranes I. Physical model*. 2003. **150**(7): p. A1008-A1015.
5. Qin, C., *Water transport in the gas diffusion layer of a polymer electrolyte fuel cell: Dynamic pore-network modeling*. 2015. **162**(9): p. F1036-F1046.
6. Zuo, Z., Y. Fu, and A.J.P. Manthiram, *Novel blend membranes based on acid-base interactions for fuel cells*. 2012. **4**(4): p. 1627-1644.
7. Cleghorn, S., et al., *A printed circuit board approach to measuring current distribution in a fuel cell*. 1998. **28**(7): p. 663-672.
8. Rajalakshmi, N., M. Raja, and K.S. Dhathathreyan, *Evaluation of current distribution in a proton exchange membrane fuel cell by segmented cell approach*. 2002. **112**(1): p. 331-336.
9. Yoon, Y.-G., et al., *Current distribution in a single cell of PEMFC*. 2003. **118**(1-2): p. 193-199.
10. Hermann, A., T. Chaudhuri, and P. Spagnol, *Bipolar plates for PEM fuel cells: A review*. 2005. **30**(12): p. 1297-1302.
11. Geiger, A., et al., *An approach to measuring locally resolved currents in polymer electrolyte fuel cells*. 2004. **151**(3): p. A394-A398.
12. Stumper, J., et al., *In-situ methods for the determination of current distributions in PEM fuel cells*. 1998. **43**(24): p. 3773-3783.
13. Hakenjos, A., et al., *A PEM fuel cell for combined measurement of current and temperature distribution, and flow field flooding*. 2004. **131**(1-2): p. 213-216.
14. Sun, H., et al., *A novel technique for measuring current distributions in PEM fuel cells*. 2006. **158**(1): p. 326-332.

15. Dong, Q., et al., *Distributed performance of polymer electrolyte fuel cells under low-humidity conditions*. 2005. **152**(11): p. A2114-A2122.
16. Shrivastava, U.N. and K. Tajiri, *Sources of current density distribution in the land-channel direction of a pemfc*. 2016. **163**(9): p. F1072-F1083.
17. Wang, Y. and K.S. Chen, *Effect of spatially-varying GDL properties and land compression on water distribution in PEM fuel cells*. 2011. **158**(11): p. B1292-B1299.
18. Deevanhxay, P., et al., *Effect of liquid water distribution in gas diffusion media with and without microporous layer on PEM fuel cell performance*. 2013. **34**: p. 239-241.
19. Eller, J., et al., *Progress in in situ X-ray tomographic microscopy of liquid water in gas diffusion layers of PEFC*. 2011. **158**(8): p. B963-B970.
20. Natarajan, D. and T. Van Nguyen, *Three-dimensional effects of liquid water flooding in the cathode of a PEM fuel cell*. 2003. **115**(1): p. 66-80.
21. He, W., J.S. Yi, and T. Van Nguyen, *Two-phase flow model of the cathode of PEM fuel cells using interdigitated flow fields*. 2000. **46**(10): p. 2053-2064.
22. Meng, H., *Multi-dimensional liquid water transport in the cathode of a PEM fuel cell with consideration of the micro-porous layer (MPL)*. 2009. **34**(13): p. 5488-5497.
23. Reum, M., S. Freunberger, and F. S. Büchi, *Measuring the Current Distribution in PEFCs with Sub-Millimeter Resolution, II. Impact of Operating Parameters*. 2009. **156**: p. B310-B310.
24. Shrivastava, U.N. and K. Tajiri, *Segmentation of Proton Exchange Membrane Fuel Cell (PEMFC) in the Land-Channel Direction*. 2014. **3**(8): p. F53-F55.
25. Paul, D.K., R. McCreery, and K.S. Karan, *Proton transport property in supported Nafion nanothin films by electrochemical impedance spectroscopy*. 2014. **161**(14): p. F1395-F1402.